This is a preprint of: Van Vuuren JH, Dippenaar MA, Van Biljon R, Van Rooy JL. 2021. Seepage Through Permeable Interlocking Concrete Pavements and Their Subgrades Using a Large Infiltration Table Apparatus. International Journal of Pavement Research and Technology. http://dx.doi.org/10.1007/s42947-021-00010-8

Seepage through permeable interlocking concrete pavements and their subgrades using a large infiltration table apparatus

Abstract

Permeable Interlocking Concrete Pavements (PICP) are being used increasingly in stormwater management. A two-year experimental study was conducted to quantify some uncertain parameters related to PICP. The study entailed the hydraulic testing of a representative volume of PICP within a specially constructed Infiltration Table Apparatus with a surface area of 10 m^2, and able to be tilted up to 6°. The study aimed to address some of the controls of infiltration into, and flow through PICP by investigating the effect of the selected construction materials and the incline of the pavements. Based on the permeability data gained on PICP, it was verified that both the choice of construction materials (in both the layer works and the sand used for fill between the bricks) and the incline of the pavements were found to affect their hydraulic properties. In general, the selection of lower permeability materials in a PICP surface layer, and/ or increasing the incline, decrease the overall permeability of the pavement.

Keywords: Permeable pavement; unsaturated flow; stormwater; urban drainage

1. Introduction

Permeable interlocking concrete pavements (PICP) have become increasingly prominent in the urban development industry's goals toward more environmentally friendly design directives, known as water sensitive urban design (WSUD) or sustainable drainage systems (SuDS). These alternatives aim to decrease anthropogenic impacts on the environment through intelligent design. As a result, permeable pavements and, in particular PICP, have seen increased application in the past 30 years (Lucke et al., 2014) as their primary function is in combatting some of the most notable issues faced by this industry related to stormwater management, water conservation, and groundwater pollution.

Common applications for PICP include interior and exterior parking areas, driveways, walkways, traffic barriers, and a host of other engineering applications which are growing each year. They can be rapidly constructed, have good load-bearing capabilities, and are fairly cost effective. However, the main reason for the increasing recent applications of PICP in WSUD and SuDS in recent years are their hydraulic properties. Their high permeabilities and hydraulic conductivities promote water ingress into the pavement instead of diverting it to surface drainage systems. They can be designed to have specific hydraulic properties as well, providing engineers and practitioners with several benefits for their designs.

PICP serves to manage stormwater. They are able to accommodate between 5 000 and 10 000 mm/hour of stormwater (Ferguson, 2006) and will naturally discharge that water at a far slower rate depending on the design. This results in reduced downslope flooding, erosional damage and surface ponding or blocked drains

(Figure 1). They act as reservoirs for large scale on-site water attenuation and storage in urban developments, with adequately designed and constructed PICP with relatively small surface areas being able to store more than 6 mm of rainfall with ease. This liberates valuable development space which would otherwise be used for on-surface storage tanks (Kelly et al., 2007). In doing this, PICP are also able to remove contaminants such as nitrates and heavy metals from water flowing through them, acting as filters and further combating groundwater pollution (Lucke et al., 2014).

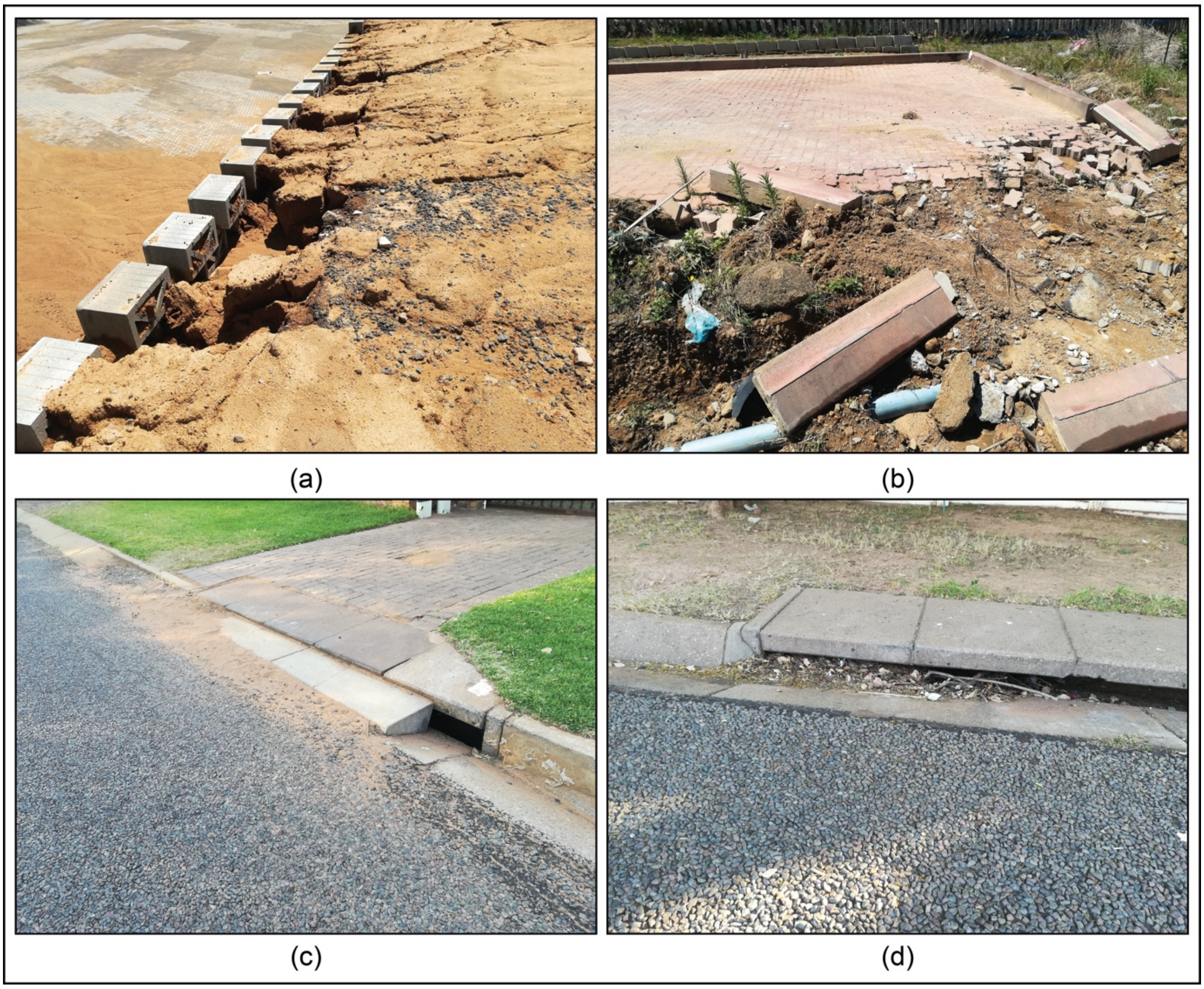

[FULL-PAGE WIDTH]

Figure 1. Examples of (a) erosional damage to retaining walls, (b) damage to interlocking pavements as a result of poor drainage and (c) and (d) stormwater drains clogged by silt and organic matter respectively.

While the many benefits of PICP have made them a popular alternative to standard interlocking concrete pavements (ICP) and other surfacing options, especially in terms of WSUD or SUDS, they are still a fairly novel development option. As a result, very little design data exist for PICP and most real-world designs are based exclusively on the experience of the engineer or professional. As such, this two-year experimental study was undertaken with the objectives of (a) addressing the controls surrounding flow into and through PICP, (b) collating and evaluating the permeable pavement data available for WSUD and SuDS, and (c) contributing to hydraulic understanding of the materials used to construct PICP.

2. Literature

2.1. Interlocking Concrete Pavements

A pavement comprises a group of layers, of differing materials, built upon a natural surface (subgrade) to create a stable area on which to operate vehicles (TRH 14, 1980; TRH 20, 1990). Common examples of pavements, based on this definition, include arterial roads, freeways, loading bays, and runways, and are intended for high traffic volumes (400 vehicles per day) and heavy axel loads (80 kN or more). Most of these pavements are sealed as water ingress into their layer works will result in instability and decrease their service lifetime. However, with the advent of WSUD and SuDS, there are a growing number of unsealed pavements, designed to suit a wider variety of requirements in urban developments as well.

From top to bottom, the layer works of almost all pavements follow a simple structure: surface, base, sub-base and selected subgrade/subgrade. Each of these layers performs a specific function and, in load-bearing pavements such as arterial roads or national freeways, must adhere to several rigorous standards such as those described in TRH 14 (1980) and TRH 20 (1990).

Standard ICP (interlocking concrete pavements) are generally less engineered and differ slightly in structure to that of load-bearing pavements. They generally consist, from top to bottom, of a surface layer of interlocking concrete bricks and a thin (25-30 mm) bedding sand layer, placed on a prepared or natural subgrade. Together, these layers also form a flexible and durable surface, but unfortunately cannot achieve the high carrying capacity of a load bearing pavement. The construction of ICP is described by Cairns (2012) and shows that while there is a great deal of preparation involved in their construction, the layer works is more simplistic and there is less emphasis on the use of standards and specifications.

Interlocking concrete pavements can be constructed to carry more intensive traffic by following the methods described in TRH 14 (1980) and TRH 20 (1990), but the surface of such a pavement would require constant maintenance and, in the process, make it financially unviable. Also, in terms of WSUD and SuDS, ICP present the same challenge as any other sealed pavement, in that they have low permeabilities and poor hydraulic conductivities.

Permeable interlocking concrete pavements (PICP) include, for instance, pervious concrete, single-sized aggregate, pervious concrete, and porous turf. Much like ICP, PICP are modular engineered surfaces that are limited to low traffic volumes and loads.

The surfaces of PICP are commonly two-part layers, consisting of interlocking, dry-cast concrete units (bricks or blocks) with a sand or fine gravel-sized material placed in the joints between them. This material, commonly known as jointing sand, consists of a sand or gravel which is free of particles measuring less than 0.425 mm known as "fines" (USDA, 2012).

In PICP the bricks themselves are not porous, but are rather designed in such a way that their geometry causes them to securely interlock while still having specified spaces between them. These spaces, in conjunction with the jointing material, provide the pathways for the infiltration of water into the pavement. Below the surface is the bedding layer which usually consists of a similar material to that used in the joints of the surface. Underlying the surface and bedding layer combination is a geotextile (a synthetic fibre-based fabric) that primarily prevents the migration of the smaller bedding layer particles into the layers below. Below are two additional compacted coarse stone layers, similar to that of load bearing pavements, namely the upper and lower sub-base. The upper sub-base layer consists of a slightly smaller particle size than that of the lower sub-base and their respective thicknesses depend on the application.

While the general structure of PICP remains consistent throughout industry, the wide variety of possible circumstances where they are applied results in differences in material selections and layer thicknesses, as well as the addition of various components such as drain pipes, meshes, silt traps and additional geotextile layers throughout the layer works, depending upon the development requirements (Technicrete, 2017). In general, there are three types of PICP that are utilised in WSUD and SuDS:

- Type Full Infiltration Pavement is designed to discharge all its water into the groundwater system. They are only used where the subgrade has a high permeability and risk to the groundwater system is minimal.
- Type-B Partial Infiltration Pavement is commonly applied where the subgrade has a moderate or low permeability and there is a risk to the soil stability due to excess water accumulation.
- Type-C Tanked or No-Infiltration Pavement is designed with an impermeable membrane below the sub-base layers to completely prevent any infiltration into the subgrade.

Permeable interlocking concrete pavements are subject to standards and specifications, such as the SuDS Manual (Woods-Ballard et al., 2007), Technicrete (2017), and National Standards for Sustainable Drainage Systems (DEFRA, 2011). These documents detail design performances, maintenance and recommended material selections for PICP layer works but, in summary, an effective PICP should have an active service lifetime of approximately 15 years and an overall permeability of approximately 4 500 ℓ/s/ha that decreases to no less than 1 250 ℓ/s/ha over the service period (Technicrete, 2017). Due to the varying application requirements, construction materials and subgrades of PICP however, there exists a large amount of deviation from material-specific standards in practice.

2.2. Unsaturated Flow

Different portions of the pavement will experience different types of flow, of which most will be under highly variable water saturation.

Unsaturated flow typically occurs as (Dippenaar and van Rooy 2019):

- Normal perching, when water is retained above a low permeability unit due to the large amount of energy required to break the suction pressures of its smaller voids
- Capillary barred perching, between two units where the higher permeability unit is found below the lower permeability one
- Imbibition, where water is drawn into a low moisture content, finer-grained unit, from one with either a higher moisture content or a larger permeability, through suction
- Shallow interflow, when water, within units of relatively low permeability, is mobilised by cohesion alone
- Percolation, when water migrates from an upper, high saturation unit or zone to a lower one through a combination of cohesion and gravity
- Unsaturated fracture flow, when water migrates between units through networks of fractures without completely wetting the surfaces of these fractures.

Unsaturated flow is complex depending on the medium (intergranular versus fractured porosity) and the distribution and succession of different media (e.g. soil overlying rock, or intergranular porosity overlying discreet openings as described by Brouwers & Dippenaar 2019), which is mimicked by vertical joints between the interlocking bricks overlying fill in PICP.

Unsaturated flow and seepage have strong horizontal controls, counteracting gravity, with typically much longer and saturated flow paths in the horizontal direction than the vertical direction. A similar type of flow behaviour was thus expected to possibly occur between the surface combination and geotextile layer in PICP (Jones et al., 2018).

2.3. Hydraulic Properties and Testing

Most of the accepted testing methods to acquire hydraulic parameters of ICP and PICP are aimed at evaluating parameters such as void ratio, porosity, density, permeability, hydraulic conductivity, or infiltration capacity (Kuosa et al., 2014). Some of the tests used in pavement construction are described by EN 1097-3 (1998) and ASTM C29 (2009), primarily evaluating the void ratio and bulk density for aggregates. ASTM C1688 (2013) and ASTM C1754 (2012), on the other hand, are also used to determine density and void content of concrete instead of aggregates.

A number of tests can be used in PICP. ASTM C1781 (2013) (single ring infiltrometer) and ASTM D3385 (2009) (double-ring infiltrometer) described tests originally intended for soils that were subsequently modified to be applicable to pavements. An example of this can be seen in studies by Hu et al., (2020) and Beeldens and Harrier (2006) where various sealants were used to prevent lateral migration of water in the pavement surface on the Single-ring and Double-ring infiltrometer tests respectively. This prevented the need for the rings to be driven into the surface as originally specified for their use on soils. . These tests rely on inducing a pressure head or flood condition above the surface of the pavement and observing gravity-driven infiltration. ASTM D5084 (2010), alternatively, makes use of a flexible wall permeameter and was also originally intended for rock and soil. ASTM D2434 (2006) applies a constant-head test to provide permeability data for the subsurface layers of a pavement, but it too was intended for another purpose, evaluating laminar flow through granular soils.

In an attempt to address the need for standardised hydraulic tests, specifically aimed at PICP in industry, several agencies are developing new tests and procedures. Two such systems have recently been formalised namely ASTM C1701, (2009) and National Centre for Asphalt Technology (NCAT) permeameter. Both have been shown to produce adequate results, but the ASTM C1701 has been reported to produce results that are up to 90% lower than the NCAT permeameter (Li et al., 2013). There have also been several studies that detail how such methods still have limitations when applied to PICP, as they are only applied to small areas of the pavement or cannot account for clogging, high volume traffic ware, upslope water sources and or the effect of incline for instance (Lucke et al., 2014).

An example of experimental procedures which test inordinately small portions of representative pavement can be seen in a study by Zhang et al., (2017) where a model of a pervious concrete surface was constructed from magnetic ball-bearings and felt in a flume that measured 2 m long, 30 mm wide and 85 mm deep. Within this flume, an extremely small (201 mm × 30 mm × 9 mm) portion was packed with a felt lining, overlain by the stainless steel ball-bearings, which do not accurately model the complexities within any pavement layer works, especially those presented by the surface texture of the aggregates. Water was then passed through this flume and the differences between the runoff volume and volume of water which flowed through the ball-bearing assembly were compared while altering several parameters such as inflow volume, outflow volumes and incline. Numerical modelling of the system was then compared to the experimental result data.

To address the issues that limit the already formalised procedures, some hydraulic test methods have been developed for use on permeable pavements, such as the Stormwater Infiltration Field Test (SWIFT) which evaluates permeability and degree of clogging. It entails placing a 25 ℓ bucket, filled with 6 ℓ of water, 60 mm above the surface of a pavement. The bucket has a 40 mm diameter hole in its base, that is plugged with a removable stopper, removed at the start of the test. The surface area that has been wet by the test is then related to the permeability of the pavement (Lucke et al., 2015).
Another study by Lucke et al. (2014) investigated a full-scale constant head and falling head testing of an area of in-situ permeable pavement. In this study, approximately 65 m^2 of pavement was isolated and subjected to

constant and falling head conditions. Pressure transducers, placed at specific locations along the periphery of the pavement, measured the change in head which was later related to the permeability of the pavement by comparing the values with data obtained from Double-ring infiltrometer tests conducted on the same pavement area. The Double-ring infiltrometer testing yielded values between 90 mm/h and 760 mm/h, while the falling head and constant head data produced variations between 46 mm/h and 259 mm/h. These full-scale tests were especially time consuming and the task of keeping the pavement section isolated proved extremely difficult.

Lucke and Beecham (2013) also presented a study which shares great commonality with this paper's model. In this study, an Infiltration Table Apparatus (ITA) was constructed in which approximately 18 m^2 of a permeable pavement could be built and subjected to simulated rainfall and upslope runoff at a rate of approximately 0.0042 m^3/min. Their ITA could also be tilted between 0% and 30%, allowing for the evaluation of the effect of incline and in each test, the entire pavement was subjected to flow but only one portion of the length of pavement could be measured at a time. Unfortunately, this study was qualitative and no permeability data for the pavement constructed within their ITA was provided. In addition, no material data was supplied apart from some basic schematic representations.

2.4. Knowledge Gaps

A PICP's performance is not governed by a single aspect of its construction but instead by a combination of factors. These factors include but are not limited to; the layer design (thickness and material), surface unit selection, topography and subgrade permeability or predevelopment condition of the pavement location. Table 1 provides a brief summary of permeability data obtained by studies conducted on PICP with different constructions and subgrade types. In general, the permeability of the pavement was higher than the predevelopment condition but the pavement performance was heavily affected by the construction material selection.

Table 1 A comparison of construction material and permeability data obtained in different studies.

Study Authors	Design Influx			Geological Origin of Pavement Construction Material				Mean Performance K (m/s)
	Storm	Rainfall Quantity	Equivalent K (m/s)	Surface	Base & Sub-base	Subgrade	Subgrade K (m/s)	
Beeldens and Herrier (2006)	1/30 year	270 l/s/ha	5.4×10^{-5}	Porphyry (Granite or Rhyolite)		Silty	NM	3.8×10^{-6}
Beeldens and Herrier (2006)	1/30 year	271 l/s/ha	5.4×10^{-6}	Porphyry (Granite or Rhyolite)		Sandy	1.03×10^{-3}	4.0×10^{-4}

Fassman and Blackbourn (2010)	1/2-5 year	1200 mm/hr	NM	NM	NM	Clay	NM	8.64×10^{-1}
Bean et al. (2007)	NM	NM	NM	NM	NM	Sandy	NM	72×10^{3}
Kumar et al. (2015)	NM	NM	NM	NM	NM	NM	NM	2.54×10^{-2}
**NM = No Mention*								

Considering the structural aspects of PICP's in literature, interesting phenomena can be noted as well. A study by Castro et al., (2007) showed that a difference in the incline at which a PICP was constructed from 0% to 2% resulted in infiltration moving from 70% in the upslope half to 70% in the middle and downslope half of the pavement instead. A similar situation was observed by Kamali et al., (2016) where it was noted that the ratio of horizontal to vertical hydraulic conductivity of the pavement changed from 0.5 to 3.5 with an increase of only 2% in incline. Despite the study's shortcomings, these results a further corroborated by the work of Zhang et al., (2017) who showed that with an increase in incline, there is a measurable increase in stormwater runoff velocity.

3. Methods

3.1. Field Testing

Double ring infiltrometer (DRI) tests detailed in ASTM D3385 (1994) were conducted to relate standard field methods with the results of the infiltration table. The double ring infiltrometer setup was slightly modified to allow it to fit in the base of conventional tests pits (0.75 m wide) and to be easily transported. The outer ring measured 300 mm high and was cut from steel tubing with an inner diameter of 300 mm and a wall thickness of 4 mm. The inner ring was made of clear acrylic with a 140 mm inner diameter, a height of 500 mm and a wall thickness of 2 mm. A steel tape measure was inserted into the inner ring to measure changes in hydraulic head.

Double-ring infiltrometer tests were conducted on a site in Brooklyn, Pretoria. The tests were conducted on this site as the in-situ material, which consists primarily of silty-sand and highly weathered quartzite gravel, is a common subgrade for pavements in South Africa. Furthermore, it is common practice for the subgrade to be prepared by excavation and compaction of the surface. For this reason, the double-ring tests were conducted in the base of two 0.7 m deep test pits excavated on the site. The tests themselves entailed driving the two rings into the base of the test pits and then adding water to the space between them to a height of 150 mm, which was maintained for the duration of the tests. The inner ring was then also filled with water to a height of 150 mm, after which testing started. The time taken for the water height in the inner ring to drop by 10 mm was measured, after which it was refilled and repeated. When the time difference between each subsequent measurement became less than 3 s, it was assumed that steady state flow had been achieved. The test was then repeated a minimum of three more times to gain the required data for the calculation of the material hydraulic conductivity. The test pits were also further investigated by hand auger and profiled by an engineering geologist according to the methods outlined by Brink and Bruin (2001)

3.2. Infiltration Table Apparatus

The information acquired during initial field tests guided the design and construction of an Infiltration Table Apparatus (ITA) for the full-scale model in the Bosun Brick (Pty) Ltd laboratory facility. The design of the ITA is described in detail by Van Vuuren (2020), and comprises a 10 m^2 stainless steel construction surface (deck) that can be tilted between 0° and 6°, upon which 8 m^2 of any PICP can be constructed provided it is less than 420 mm in height. A water reservoir supplies water (Q_{IN}) to the pavement by sheet flow through a slot cut across the upper end. Tempered glass measuring 9 mm in thickness bind the left and right sides of the pavement constructed on the deck. An adjustable steel divider bounds the lower side of the pavement at the 4 m mark (Figure 2a).

(c)

[FULL-PAGE WIDTH]

Figure 2. Experimental setup showing the (a) design specifications of the ITA; (b) ITA as constructed; (c) supply tank; and (d) the collection tank, outlet meters and the submersible pump used to recycle water in the ITA.

The deck itself is 2 m wide and 6 m long. 6 mm wide slots are cut into the deck, perpendicular to the direction of flow, at 191 mm and 132 mm intervals across the width. Slots are spaced 1 m apart with 10 mm steel rods welded into these slots in a v-shape to prevent subsurface flow from moving from one linear meter of pavement to the next. Catch trays (outlet bins) that transport pavement outflow (Q_1-Q_5) to flow meters below the slots.

The steel divider at the 4 m mark allows for the measurement of runoff (Q_5) in real time. At the midpoint of the ITA, an axel and bearings allow for tilting of the entire apparatus by means of scaffolding jacks and a 4 000 kg hand operated block-and-tackle at its upper end (Figure 2b).

Water is supplied to the ITA by an elevated 1000 ℓ (1 m^3) supply tank (Figure 2c) connected to the reservoir of the apparatus via PVC tubing and three Elster Kent V100 PSM water meters. These water meters provide the Q_{IN} value for the experiments and are furthermore referred to as "inlet meters". Ball-cocks are installed between the inlet meters and the apparatus reservoir to allow for a variable Q_{IN}, by partially or completely closing one or more of them as well as to start and end tests. Once the ITA reservoir is filled, any additional water will flow out of its slot and onto the pavement being tested. Water that flows through or over the pavement on the deck then exits the ITA and into the outlet bins which contain a 0.3 mm thick layer of polyester non-woven filter media to prevent clogging of downstream equipment.

The media have an aperture small enough to retain particles 0.4 mm and larger. Water collected in the outlet bins then flows through more PVC tubing and finally via five Madalena DS TRP flow meters (outlet meters) before being collected in the bottom half of another 1 000 ℓ (1 m^3) collection tank (Figure 2d). The outlet meters are monitored by a GoPro® camera mounted above them in real-time and would provide permeability data for the pavement being tested (Q_1-Q_5). A submersible pump then moves the water from the collection tank to the supply tank for reuse which would allow tests to be conducted for any duration of time.

3.3. Initial ITA Model Design

Based on the field data collected, a Full-scale Model was constructed, consisting of 3.36 m^3 of Full Infiltration PICP as a representative volume which would be subjected to hydraulic testing within the ITA.

Testing of the Full-scale Model considers many variables including, but not limited to, layer materials, layer thickness, the packing orientation of the interlocking bricks, incline, volume of water influx, type of influx (sheet flow vs. simulated intermittent rainfall), and even the effect of the presence of each individual layer. A series of preliminary tests were conducted in an attempt to reduce ineffective or redundant variables. To accomplish this, generic layer works (GLW) were selected, constructed and subjected to testing in an iterative manner.

The GLW consisted of six layers constructed in consecutive stages in the ITA, with the natural subgrade being represented by the deck, as follows (Figure 3):

- Bosun Waterwise® bricks in a specific pattern for the surface layer (Figure 3c)
- No fines sand (P-Type 1) for the jointing material/ other sand
- A 30 mm thick layer of P-Type 1 sand for the bedding layer
- Bidum® A2 for the geotextile layer
- A 150 mm thick layer of 6 mm crushed quartzite for the upper sub-base layer

This is a preprint of: Van Vuuren JH, Dippenaar MA, Van Biljon R, Van Rooy JL. 2021. Seepage Through Permeable Interlocking Concrete Pavements and Their Subgrades Using a Large Infiltration Table Apparatus. International Journal of Pavement Research and Technology. http://dx.doi.org/10.1007/s42947-021-00010-8

- A 150 mm thick layer of 20 mm crushed quartzite for the lower sub-base layer.

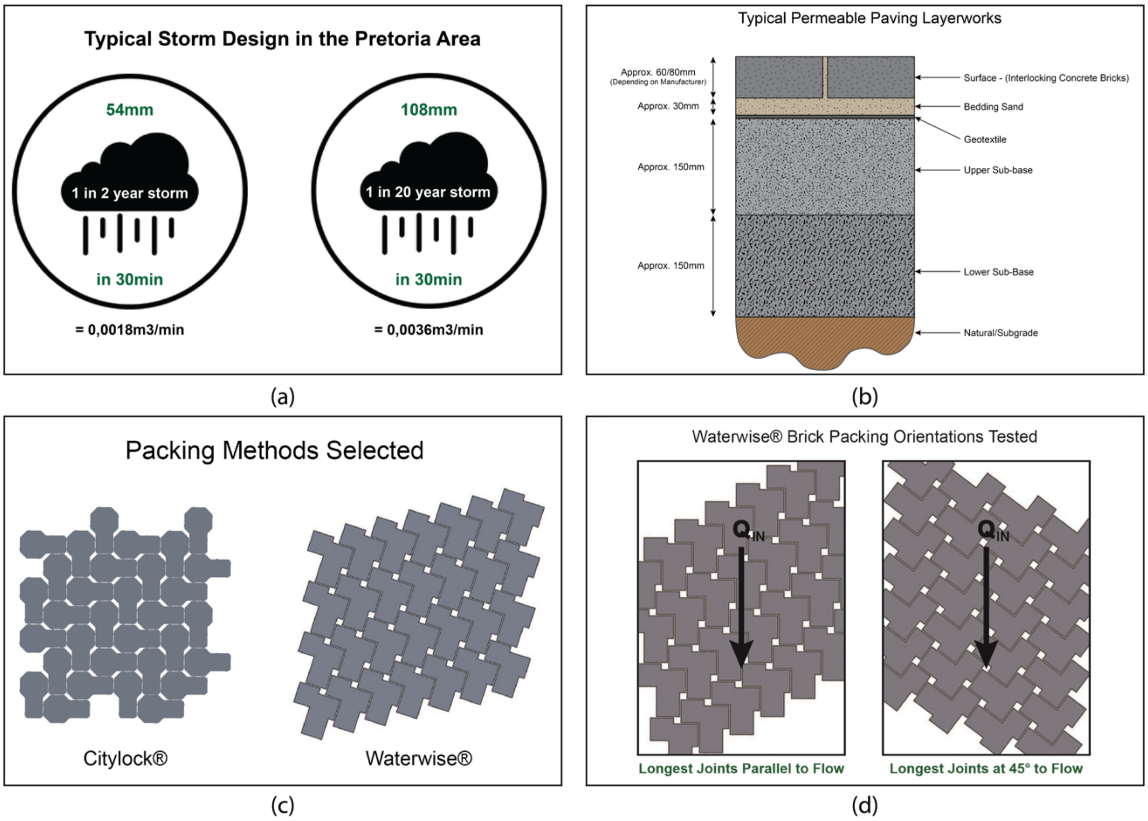

[FULL-PAGE WIDTH]

*Figure 3. Schematic representation of the (a) water influx in the Full-scale Model; (b) model layer works; (c) packing orientations selected for the products used in the model; and (d) concrete brick orientations investigated during the model design phase (*Van Vuuren 2020*).*

Preliminary testing was conducted in three stages as some variables were suspected of having little to no effect on overall PICP performance. The first stage considered the effect that each separate layer has on PICP performance; the second looked at the effect of a change in the orientation of the bricks in the surface layer; and the third considered the effect of incline on the performance of PICP.

The first stage was conducted by constructing the entire GLW in the ITA, one layer at a time, and hydraulically testing the system after each subsequent addition. When only the surface layer was present in this stage, it was placed on a 15 mm thick layer of 6 mm gravel. This was done to produce a level surface, as the 10 mm rods welded to the deck caused misalignment of the bricks without it. In addition, the surface layer was tested several times during this stage, once without any jointing material and subsequently with a range of different materials. The results of this stage were recorded for comparison with those of the field tests and subsequent stages.

The second stage entailed repacking the surface layer of the full GLW with the bricks horizontally rotated by 45° relative to their original orientation, without changing their packing method or pattern. In the first stage, the long joints of the bricks were orientated parallel to the direction of surface flow, and in the second the long joints were placed at 45° to flow. Again, the results of this stage were recorded for comparison to the previous and subsequent stages of testing. As the first and second stages did not consider the effect of incline, all of their tests were conducted with the ITA inclined to 2.5°, influx volume at maximum Q_{IN} and a duration of approximately 10 min for each test (Figure 3d).

The third and final stage of preliminary testing consisted of constructing the full GLW with the bricks in the surface layer returned to their original position as in the first stage and then subjecting the pavement to hydraulic testing at inclines of 0° (0%), 2.5° (3.5%) and 5° (7.8%) respectively. Testing of the GLW at each incline was conducted at maximum Q_{IN} for approximately 10 minutes. As before, the results of each test were recorded for comparison with the previous and subsequent stages. The results from these preliminary tests were used to design the Full-scale Model.

3.4. Full-scale Model Design

The design of the Full-scale Model centred around three principles, namely the quantity and mechanism of water influx onto the PICP, the construction materials used within it, and the incline of the PICP's operation (Figure 3).

3.4.1. Influx mechanism

Influx as sheet flow was selected for the Full-scale Model as it closely resembles what the lowest portion of sites encounters during peak flow. As for the volume of such flow events, common practice dictates designing for the influx experienced in the 1 in 20-year storm. In the Pretoria region of South Africa, heavy rainstorms typically dispense 54 mm of rain over a 30 min period, implying the maximum possible flow rate that the ITA could produce is Q_{IN} = 0.027 m^3/min, which is much higher than typical values for this region (Figure 3a).

3.4.2. Layer works

In terms of the layer works of the Full-scale Model, the selection of materials and layer thicknesses were made according to guidelines described in Technicrete (2019) and TRH14 (1980) (Figure 3b). Starting at the top, the surface layer consisted of interlocking concrete bricks and jointing material as in the GLW but, from information gained in the preliminary tests, it was decided to alternate only the brick products, jointing material and bedding material throughout the testing procedure. Many manufacturers and products were considered for use in the surface layer but testing the large variety available would have been unviable in the scope of this project. As such, two products were selected, namely Bosun's Waterwise® and Citylock® bricks (Figure 3c). These two closely resemble the physical aspects of the majority of those commonly applied in industry, but also differ from one another enough to verify whether brick geometry has an influence.

These two products both measured 60 mm high and were in the same price category as the majority of other products available. Their geometries furthermore allowed for the variation of the surface permeability depending on the packing method. While this was useful for the alteration of the testing procedure if needed, only one packing method was selected as a result of data gained from the preliminary tests.

For the bedding and jointing material, practitioners and best practice guidelines prescribed certain requirements on these materials for PICP (Technicrete 2019). The Plasticity Index (PI) should be zero and all particles should be larger than 0.425 mm in diameter. Chemistry of bedding and jointing material was rarely addressed. While a number of sands throughout South Africa would meet these requirements, their composition and thus chemistry would vary between regions To ensure repeatability, a class system for these materials was developed that consists of five particle type (P-Type) categories and one material satisfying each class was selected for testing (Figure 4). The bedding layer was kept at a constant thickness of 30 mm for all tests and the material selected it, was also used as the joining material for that test for uniformity.

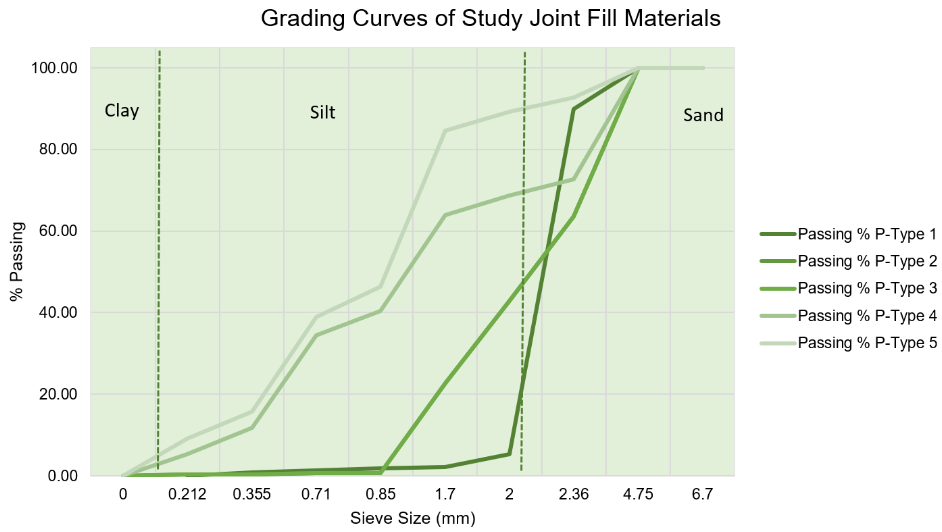

[3/4 PAGE WIDTH]

Figure 4. Grading curves for the sands selected in the P-Type classes for this study.

P-Type 1 or "No Fines Sand" is a washed, sieved, silica-rich, chemically stable sand, with 80% of particles by weight falling between 1.0 and 5.0 mm in diameter. These sands are commonly only available from specialist suppliers and are produced with a high degree of particle size control, making them less affordable than others. They are however strongly recommended by professionals for use in PICP and served as the ideal bedding and jointing material in this study.

P-Type 2 or "No Fines Sand 2" is a slightly more affordable variant to the P-Type 1 due to a lower degree of particle size control but it was also only available from a specialist supplier. It consists of a washed, sieved, silica-rich, chemically stable sand, with 80% of particles by weight falling between 0.85 and 5.0 mm in diameter.

P-Type 3 is a "Crushed Stone" which consists of a sand-like material produced by crushing quarried rock and sieving it to a degree such that 80% of particles by weight falling between 0.4 and 2.0 mm in diameter. This class of material was selected as it was far more affordable than P-Types 1 and 2, but chemical stability was a concern. A P-Type 3 produced from an igneous rock such as granite or a chemical sediment such as dolomite would weather more rapidly over time than others, producing clay minerals or completely dissolving in slightly acidic water respectively. For this reason, a quartzitic parent P-Type 3 material was used.

P-Type 4 or "Coarse Building Sand" class is selected to inform on the use of highly affordable alternatives to the other material classes. It consists of a silica-rich, well-graded, general purpose building sand with a low clay content and 80% of particles by weight falling between 0.2 and 5.0 mm in diameter. This is done because many developments often do not make use of the full performance of PICP, or simply just do not have the required funding.

P-Type 5 or "Fine Building Sand" consists of a poorly sorted, general purpose building sand with 80% of particles by weight falling between 0.2 and 2.36 mm in diameter. This type of material is commonly mixed with coarse aggregates and cement in the production of concrete and was readily available and extremely affordable. This class represented the worst possible material selection for PICP.

A single geotextile layer consisting of A2 Bidim® was placed below the surface and bedding layers for any given test. The geotextiles are nonwoven, needle-punched, continuous filaments of polyester fabric. Its average pore size and hydraulic conductivity are 170 um and 4.2×10^{-3} m/s respectively.

Beneath the geotextile is two additional layers of crushed stone measuring 150 mm each forming the upper and lower sub-base layers. The upper consisted of a 6 mm crushed quartzite while the lower of 20 mm crushed quartzite respectively. Quartzite is selected as it is a readily available and chemically stable material while also being highly recommended by practitioners for its high strength and durability.

3.4.3. Incline

Pavements are mostly designed to have the minimum possible incline as heavy vehicles have low incline traversal limits. Inclines of as little as 2° or 3.5% extending over a long area of pavement can have serious implications on downstream drainage systems. Many developments are however limited by budget and available space and so high incline areas of pavement are unavoidable. For these reasons, testing of each layer works combination was conducted at inclines of 0° (0%), 2.5° (3.5%) and 5° (7.8%).

3.5. Full-scale Model Testing

Testing of the Full-scale Model was iterative, and the first step of the testing procedure was to prepare the ITA and the selected layer works for that specific test by setting the ITA to an incline of 0°, and constructing the required layer works within it according to best practice guidelines as far as possible (Technicrete, 2019 and TRH14, 1980). Once complete, the apparatus's reservoir was filled by opening the valve ahead of the supply tank, followed by the tree ball-cocks at the inlet meters until water started exiting the reservoir through the slot cut in it. The three ball-cocks were then immediately closed and their readings were taken. These readings were taken to be the starting volume of that test. Next, the valves after the outlet meters were opened allowing the ITA to drain fully of any water that may have built up in the ITA drainage system from a previous test or while filling the apparatus reservoir. Readings were then recorded from the outlet meters and this was taken to be the starting volumes at the outlet meters for that specific test.

Once the preparation phase was complete, testing was commenced by opening all three ball-cocks at the inlet meters fully, starting a stop watch and the recording of the GoPro® camera simultaneously. Any water that entered the reservoir after preparation, flowed out through its slot and onto the pavement being tested, migrating through it if possible and exiting the ITA through the slots in the deck and their corresponding catch trays to be recorded by the outlet meters. Readings were captured in real time by the camera, but manual readings were also taken every 5 min as a precaution and for determination of the test termination time. All tests were terminated once steady state flow was achieved, taken to be when all outlet meter readings differed by the same amount, every 5 min, to two decimals (Discharge, Q (m^3/min)).

Once steady state flow was achieved, the test was terminated by closing the tree ball-cocks at the inlet meters, stopping the stopwatch and the camera recording, and taking readings of all the flow meters of the ITA. These readings were taken to be the end volumes and the differences between them, and the start volumes were taken to be the total volume flux experience by that PICP for that test. After allowing the ITA to drain completely, its incline was adjusted to the next required interval and the entire procedure was repeated again. Once testing of that layer works at all three incline intervals was complete, the ITA was adjusted to 0° for construction and testing of the next layer works. This methodology was applied to the following layer works combinations at all three selected inclines while keeping the geotextile layer, upper sub-base and lower sub-base constant:

1) Waterwise® brick surface with P-Type 1 jointing and bedding material
2) Waterwise® brick surface with P-Type 2 jointing and bedding material
3) Waterwise® brick surface with P-Type 3 jointing and bedding material
4) Waterwise® brick surface with P-Type 4 jointing and bedding material
5) Waterwise® brick surface with P-Type 5 jointing and bedding material
6) Citylock® brick surface with P-Type 1 jointing and bedding material
7) Citylock® brick surface with P-Type 2 jointing and bedding material

8) Citylock® brick surface with P-Type 3 jointing and bedding material
9) Citylock® brick surface with P-Type 5 jointing and bedding material.

4. Results

4.1. Field Testing

The soil profiles of the two test pits excavated on the site in Pretoria comprised primarily of a thin fill layer at the surface, followed by a silty clayey sand containing abundant highly weathered quartzite gravel until, there was refusal with the hand auger on a cobble or large gravel particle in both cases. Nine double ring infiltrometer test were conducted on HA01 and six on HA02 (3). Infiltration rates were all in the order of 0.25-0.63 cm/s.

Table 2. Double ring infiltrometer test results for HA01 and HA02.

Test Pit	Test	Reading (s)	Infiltration Rate (cm/s)	Infiltration Rate (m^3/s)
HA01	T1	25	0.40	6.16E-06
	T2	24	0.42	6.41E-06
	Steady State Flow			
	T3	32	0.31	4.81E-06
	T4	32	0.31	4.81E-06
	T5	31	0.32	4.97E-06
	T6	30	0.33	5.13E-06
	Average	31.25	0.32	4.93E-06
HA02	T1	21	0.48	7.33E-06
	T2	39	0.26	3.95E-06
	T3	25	0.40	6.16E-06
	Steady State Flow			
	T4	17	0.59	9.06E-06
	T5	16	0.63	9.62E-06
	T6	18	0.56	8.55E-06
	T7	20	0.50	7.70E-06
	T8	22	0.45	7.00E-06
	T9	19	0.53	8.10E-06
	Average	18.67	0.54	8.34E-06

This type of material is often used as a subgrade in pavements throughout South Africa once compacted and so, the deck of the ITA had to be designed with slots large enough to have a higher permeability than this material and any of those in the Full-scale Model. This was done because the deck could limit the system permeability if any one layer in the model had a lower permeability than it did. Additionally, the resulting high design permeability of the deck meant that all downstream drainage systems and flow meters had to be large enough to accommodate the exiting flow, without retarding it in any way as well. Lastly, if a silty-sand could display such high permeabilities, it was reasonable to assume that the permeability of PICP constructed in the ITA would be at least one order of magnitude greater. This means that saturating such a high permeability unit would require immense flow rates and for that reason, the maximum possible Q_{IN} value of 0.027 m^3/min was selected for use in the Full-scale Model.

4.2. Full-scale Model Design

The first few iterative tests were conducted with only the surface layer present in the ITA. All the flow was attenuated within the first linear metre of pavement and only the flow meter connected to Q_1 displayed a reading and accounted for 100% of the volume that entered the ITA. This was the case for the surface layer consisting of Waterwise® bricks alone and the bricks with a P-Type 1 jointing material. The subsequent tests carried out on the GLW adding the bedding layer, geotextile and upper sub-base layers respectively produced remarkably similar behaviour, with little to no increase in the discharge from other portions of the pavement (Figure 5a).

The first time a change was noticed was when the lower sub-base was added to the GLW. It caused an increase in the discharge measured at Q_2, most likely due to the greater vertical distance that water had to traverse before exiting the pavement. This increase was an order of magnitude lower than the flow measured at Q_1, which implied that there was development of a lateral flow component within the pavement due to the testing incline of 2.5°, rather than the addition of the lower layer. Furthermore, there was no runoff (Q_5) or other discharge variation measured during these tests, implying that no single layer within PICP is solely responsible for its hydraulic performance. The individual layers rather perform structural roles such as filtration and increasing the bearing capacity and storage capacity of the pavement. Logically, a drastic change in layer thickness or material selection for PICP would change its performance and are strongly not recommended by practitioners and literature but these tests demonstrated that slight variations in particle size and layer thicknesses are permissible without a negative impact on the pavement's performance.

The next iterative test of the model design phase was aimed at a common occurrence in industry, namely the selection of an inferior bedding and jointing material. A lack of experience, material availability and/or budget constraints can often lead to poor selections of these materials and, as the surface is the entry point for water into the PICP, it stands to reason that such a selection could limit the performance of the entire system, regardless of the permeability of the lower layers. To verify this and investigate how drastic the variations in performance could be due to such a change, this iterative test was conducted with a P-Type 5 bedding layer and jointing material in the GLW. The result was a sharp increase in discharges measured from Q_2-Q_4 and a decrease in discharge at Q_1 but most notably, for the first time during the iterative testing, runoff (Q_5) occurred. This implied that one of the most influential portions of PICP layer works was the combination of concrete bricks, jointing material and the bedding layer that makes up its surface combination (SC). For this reason, the type of material and brick product selection were thoroughly investigated in the Full-scale Model (Figure 5b)

This is a preprint of: Van Vuuren JH, Dippenaar MA, Van Biljon R, Van Rooy JL. 2021. Seepage Through Permeable Interlocking Concrete Pavements and Their Subgrades Using a Large Infiltration Table Apparatus. International Journal of Pavement Research and Technology. http://dx.doi.org/10.1007/s42947-021-00010-8

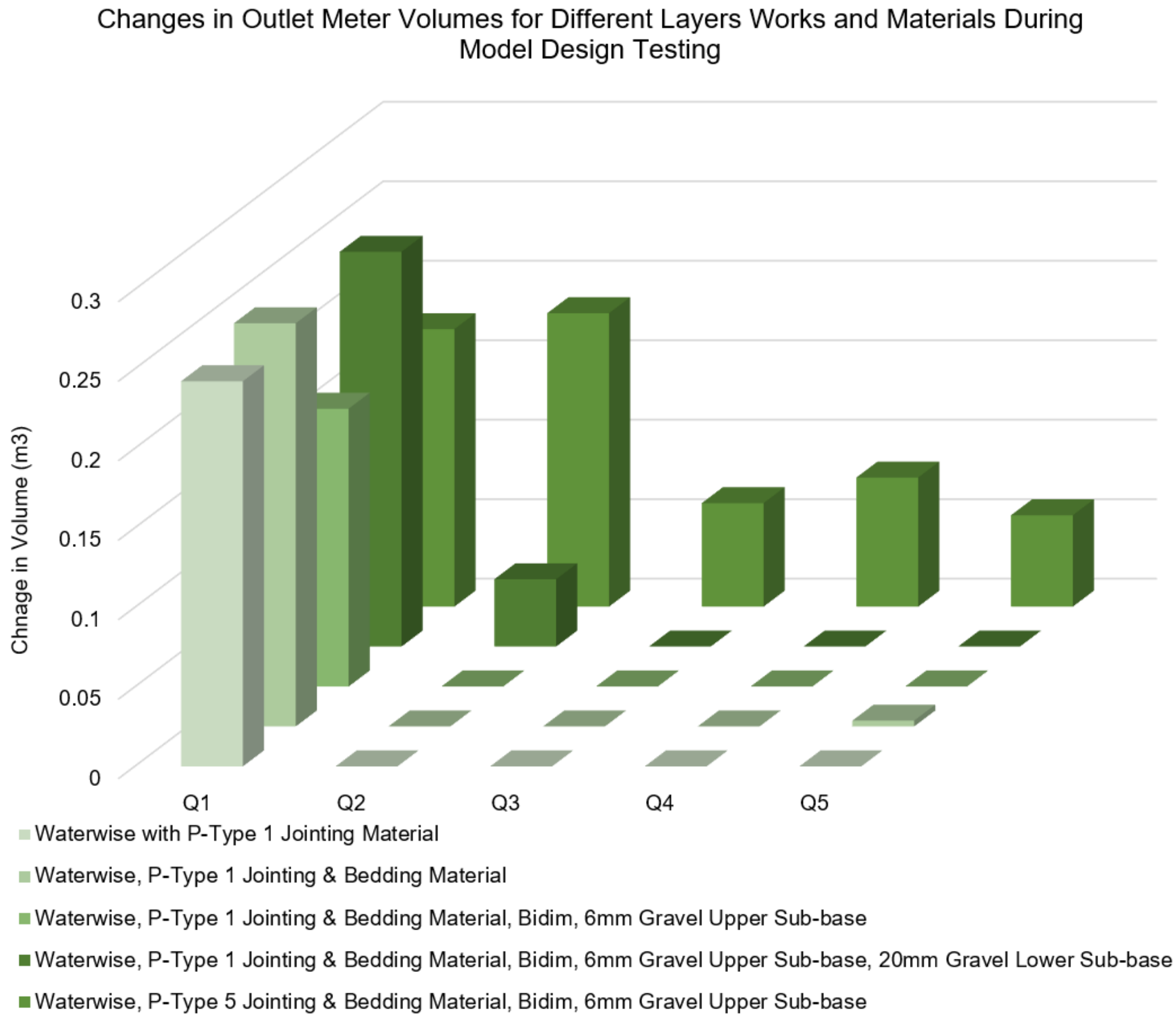

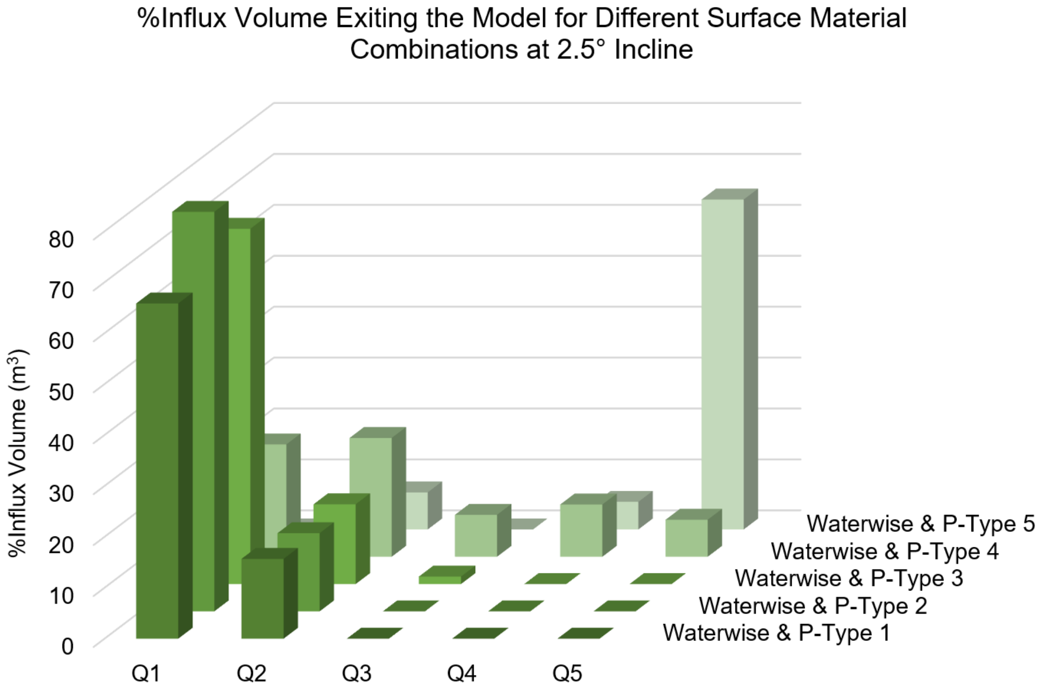

This is a preprint of: Van Vuuren JH, Dippenaar MA, Van Biljon R, Van Rooy JL. 2021. Seepage Through Permeable Interlocking Concrete Pavements and Their Subgrades Using a Large Infiltration Table Apparatus. International Journal of Pavement Research and Technology. http://dx.doi.org/10.1007/s42947-021-00010-8

Figure 5.(a) Comparison of exit volume changes at each point for the model design tests for different layers of the GLW; (b) exiting percentages of influx volume at each point for different surface material combinations in the Full-Scale Model at a 2.5° incline.

Following that, another iterative test for the model design phase was conducted looking at a structural property that was suspected to have an effect on PICP performance, namely the orientation of the bricks in the surface layer. The suspicion was that PICP with the longest joints of their bricks parallel to the downslope flow direction, would experience greater downslope migration of water before infiltration than those with the longest joints at an angle to the flow direction. This was because the aligned joints were suspected to provide preferential pathways for downslope flow while misaligned joints would produce longer downslope flow pathways, promoting infiltration instead. No discernible change in the system performance between the two instances was noted, and so the orientation of the bricks in the surface layer was not further investigated in the Full-scale Model.

Lastly, the iterative testing of the model design phase testing looked at the effect of incline on PICP performance by subjecting the full GLW to inclined testing in the ITA and the results are shown in Figure 6. As before, nearly all water entering the ITA from the reservoir was attenuated within the first linear metre of pavement, but as incline was increased, there was a notable decrease in discharge from points Q_1 and Q_2. This implied that water tended to move further and further downslope before traversing the vertical thickness of the pavement as incline was increased with the sharpest change occurring at an incline of 5°, supporting the finding that a there was development of a lateral flow component with an increase in incline. For this reason, it was decided that incline be deeply investigated in the Full-scale Model.

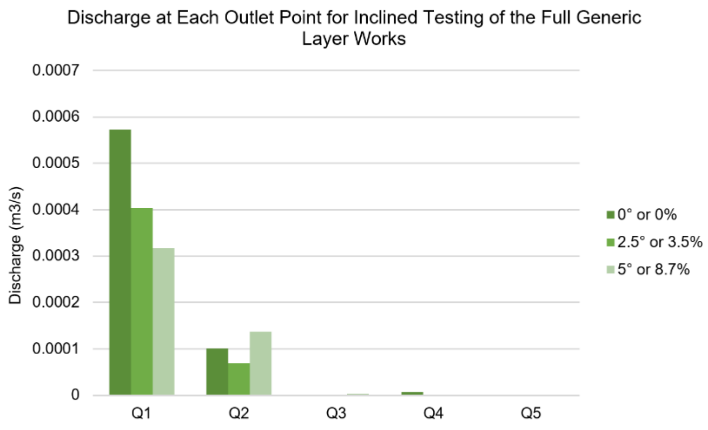

[SINGLE-

Figure 6.Discharges at different exit points of the Infiltration Table Apparatus as incline increased.

4.3. Full-scale Model

This is a preprint of: Van Vuuren JH, Dippenaar MA, Van Biljon R, Van Rooy JL. 2021. Seepage Through Permeable Interlocking Concrete Pavements and Their Subgrades Using a Large Infiltration Table Apparatus. International Journal of Pavement Research and Technology. http://dx.doi.org/10.1007/s42947-021-00010-8

Before addressing the specific results of the Full-scale Model, it is important to understand their presentation. The results for these tests, shown in Appendix A, are presented in 5 min time intervals, starting at 10 min. The reason for this is that almost every test reached steady state flow within 10 min, as demonstrated in 4 and Figure 7 which shows the 1 min interval results of a test conducted on the Full-scale Model with a P-Type 1 and Waterwise® SC at an incline of 2.5°. It is clear that steady state flow occurs between 2 and 3 min in this test as the difference between each volumetric reading becomes very small. Additionally, the mean discharges (QMean) shown are calculated based on steady state flow data only. This eliminates incoherencies that may be introduced by the model reaching steady state flow from zero flow and the period directly after the ball-cocks at the inlet meters are closed and the model is draining freely. Lastly, all SC containing Waterwise® bricks and P-Type 1 material are displayed as such while other SC were allowed more time to discern any possible differences.

Table 3. Short interval test results for a Waterwise® and P-Type 1 combination layer works of the Full-scale Model (2018/09/06; incline 2.5° or 3.5%).

Time (min):	**Inlet Meters (m^3)**			**Outlet Meters (m^3)**									
	1	**2**	**3**	**Q_1**	**Discharge Q_1 (m^3/min)**	**Q_2**	**Discharge Q_2 (m^3/min)**	**Q_3**	**Discharge Q_3 (m^3/min)**	**Q_4**	**Discharge Q_4 (m^3/min)**	**Q_5**	**Discharge Q_5 Runoff (m^3/min)**
0	3.30763	4.3863	2.77682	0.64	0	0.31758	0	0.2441	0	0.46075	0	1.07115	0
1	-	-	-	0.6405	0.00362	0.31758	0	0.2441	0	0.46075	0	1.07115	0
2	-	-	-	0.66223	0.02173	0.32114	0.00356	0.2441	0	0.46075	0	1.07115	0
3	-	-	-	0.68618	0.02395	0.3256	0.00446	0.2441	0	0.46075	0	1.07115	0
4	-	-	-	0.70922	0.02304	0.32948	0.00388	0.2441	0	0.46075	0	1.07115	0
5	-	-	-	0.73215	0.02293	0.33315	0.00367	0.2441	0	0.46075	0	1.07115	0
6	-	-	-	0.75377	0.02162	0.33681	0.00366	0.2441	0	0.46075	0	1.07115	0
7	-	-	-	0.77548	0.02171	0.34043	0.00362	0.2441	0	0.46075	0	1.07115	0
8	-	-	-	0.79821	0.02273	0.34428	0.00385	0.2441	0	0.46075	0	1.07115	0

9	3.4205	4.52323	2.84195	0.82011	0.0219	0.34829	0.00401	0.2441	0	0.46075	0	1.07115	0
End				0.88521	0.0651	0.35992	0.01163	0.2441	0	0.46075	0	1.07115	0
(Q_{Mean}) (m^3/min)	**0.011287**	**0.013693**	**0.06513**		**0.020358889**		**0.0034122**		**0**		**0**		**0**

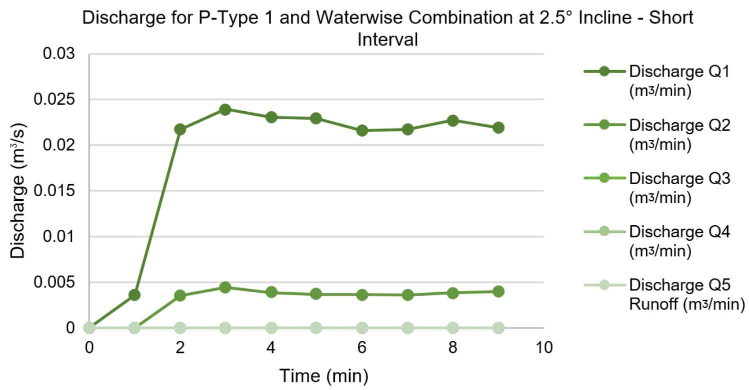

[SINGLE-COLUMN WIDTH]

Figure 7.Short interval discharges at different points of Full-scale Model with a Waterwise and P-Type 1 combination layer works.

4.4. The Effect of Surface Materials

The model design phase showed that in general, the SC of PICP has the greatest influence on its permeability but to ascertain exactly what that effect is, incline must be eliminated as a variable. Thus, consider the results of the tests conducted at 2.5°only . An incline of 2.5° is great enough to accentuate the downslope effects of the material choices on PICP permeability by allowing for the development of a lateral flow component, without it being dominant over the vertical. The results for these tests are summarised in 5 and Figure 5b along with their corresponding permeability values and percentage improvement according to Eq. 2. Firstly, it can be seen that changing the brick product alone has an effect on PICP performance as the use of Citylock® bricks increased the permeability (Kp/m) of the pavement by between 5% and 48% as opposed to an identical layer works containing Waterwise® bricks instead. Due to the time constraints of the project however, a SC containing Citylock® and P-Type 4 material could not be tested but its permeability can be estimated to be within 5% of that of a SC containing Waterwise® and P-Type 4 material, using the trends in the data of other combinations.

Table 4. Maximum discharge and permeability values per linear meter of pavement for different surface material combinations at 2.5° incline.

Product	**Sand Type**	**Maximum Q_{Mean} (m^3/min)**	**Maximum $K_{p/m}$ (cm/s)**	**Percentage Decrease vs. P-Type 1**	**Percentage Improvement vs. Waterwise**
Citylock	P-Type 1	0.028702	2.39E-02	-	48.0%
	P-Type 2	0.020015	1.67E-02	30.27%	2.0%
	P-Type 3	0.020185	1.68E-02	-0.85%	4.1%
	P-Type 4	Not Tested	±8.00E-03 Expected	52.44%	NA
	P-Type 5	0.0018075	1.51E-03	81.17%	5.2%
Waterwise	P-Type 1	0.0193876	1.62E-02	-	-
	P-Type 2	0.019626	1.64E-02	-1.23%	-
	P-Type 3	0.019395	1.62E-02	1.18%	-
	P-Type 4	0.009344333	7.79E-03	51.82%	-
	P-Type 5	0.001718	1.43E-03	81.61%	-

$$K_{p/m} = \frac{Q_{Mean}(\mathrm{m^3/s})}{\text{Surface Area of 1 linear m of pavement }(\mathrm{m^2})} \times 100\ \mathrm{cm/m} \quad (2)$$

Where:

$K_{p/m}$ = Permeability of linear meter of pavement 1, 2, 3 or 4 (Runoff is not considered)

Q_{Mean} = The mean discharge of the linear meter of pavement in question

Changing the jointing and bedding material in the SC of the Full-scale Model had an even greater effect on its permeability. Materials from P-Type 1, 2 and 3 classes were the most effective, attenuating approximately 70% of water within the first linear metre (Q_1) of pavement and producing no runoff (Figure 5b). By comparing their permeabilities (Kp/m) to typical values (e.g. Powers, 1992), it can be seen that these materials result in the pavement performing similarly to well graded or uniform sands and could easily cope with the flow rates dispensed by 1 in 20-year storms. There was a drastic decrease in the permeability of the model when a P-Type 4 material was used, with only 50% of the water entering the ITA being attenuated within the first linear metre of pavement (Q_1). An increase of between 8% and 10% was seen in the volumes attenuated at points Q2, Q3 and Q_4, with 7% exiting the model as runoff.

When runoff occurs, it implies a critical failure in the performance of PICP and in well-constructed pavements, should only occur in extreme circumstances such as 1 in 100-year storms. This meant that, despite the model being comprised almost entirely of highly permeable units such as the upper and lower sub-base layers, a poor material choice in the SC limited the permeability of the pavement to that of a silty sand (Powers, 1992), giving further support to the finding that the surface of PICP is the most critical portion of its layer works.

Lastly, when a P-Type 5 material was used in the SC of the model, the system permeability became extremely low. Between 60% and 80% of water entering the ITA exited as runoff while the remainder was infiltrated

This is a preprint of: Van Vuuren JH, Dippenaar MA, Van Biljon R, Van Rooy JL. 2021. Seepage Through Permeable Interlocking Concrete Pavements and Their Subgrades Using a Large Infiltration Table Apparatus. International Journal of Pavement Research and Technology. http://dx.doi.org/10.1007/s42947-021-00010-8

between points Q_1, Q_2, Q_3 and Q_4 in amounts between 0% and 7%. From this, two principles governing PICP permeability can be derived namely; the permeability of the entire pavement will be limited by the SC if it has a lower permeability than that of the layers below and the permeability of the pavement is determined by the intrinsic material properties of each layer such as void content, porosity, density and permeability rather than the structural properties such as layer thickness.

4.5. The Effect of Incline

Considering all results obtained from the Full-scale Model testing, a general trend can be seen: as incline increases, permeability per linear metre ($K_{p/m}$) of the pavement decreases. The results for the model with SC containing Waterwise® and Citylock® bricks are summarised in terms of their maximum mean discharge per linear metre (Max Q_{Mean}) in Figure 8a, Figure 8b and 6.

Considering firstly the results for Waterwise® SC, it can be seen that regardless of the choice of bedding and jointing material, the discharge at each point (excluding Q_5) decreased with increasing inclines. The effect of incline on the model with these SC was aggravated by low permeability bedding and jointing materials such as a P-Type 5, which caused the difference in discharge per linear metre to decrease by two orders of magnitude between 0° and 5° inclines, shifting permeability behaviour from a silty sand to a low-plasticity silt respectively (Powers, 1992). The same could be seen in results obtained from the model with SC containing Citylock® bricks and again, the P-Type 5 bedding and jointing material caused a one order of magnitude difference in discharge per linear metre between 0° and 5° and a behavioural change from a silty sand to a clayey sand (Powers, 1992).

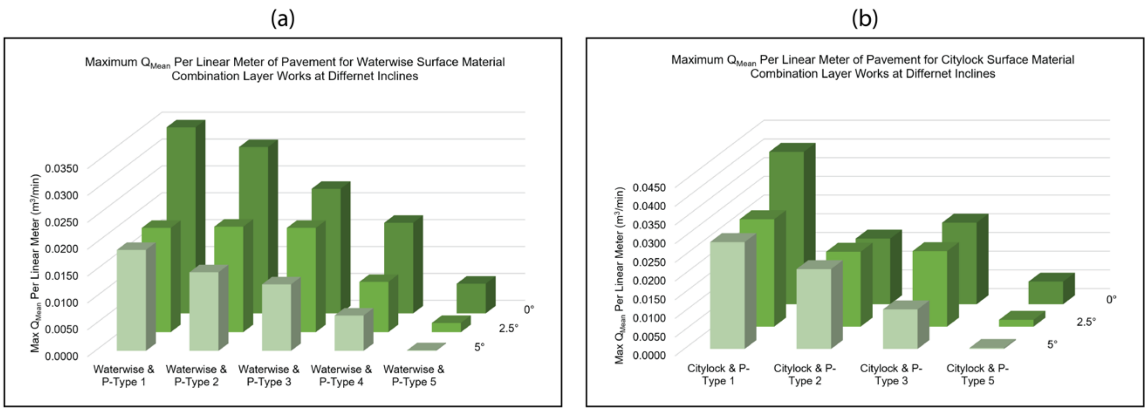

Figure 8. Maximum mean discharge per linear meter of pavement for (a) Waterwise and (b) Citylock containing surface material combination layer works in the Full-scale Model at different inclines.

Table 5. A data comparison of Full-scale Model layer works with surface combinations containing Waterwise® bricks at different inclines.

Surface Product	Incline	Parameter	P-Type 1	P-Type 2	P-Type 3	P-Type 4	P-Type 5
Waterwise®	0°	Max Q_{Mean} (m^3/min)	0.0346	0.0309	0.0232	0.0169	0.0055
		Max $K_{p/m}$ (cm/s)	2.89E-02	2.58E-02	1.93E-02	1.40E-02	4.60E-03
	2.5°	Max Q_{Mean} (m^3/min)	0.0194	0.0196	0.0194	0.0093	0.0017
		Max $K_{p/m}$ (cm/s)	1.62E-02	1.64E-02	1.62E-02	7.79E-03	1.43E-03
	5°	Max Q_{Mean} (m^3/min)	0.0188	0.0146	0.0124	0.0066	0.0001
		Max $K_{p/m}$ (cm/s)	1.57E-02	1.22E-02	1.03E-02	5.49E-03	9.55E-05
Citylock®	0°	Max Q_{Mean} (m^3/min)	0.0407	0.0175	0.0218	Not Tested	0.0060
		Max $K_{p/m}$ (cm/s)	3.39E-02	1.46E-02	1.82E-02	Not Tested	5.04E-03
	2.5°	Max Q_{Mean} (m^3/min)	0.0287	0.0200	0.0202	Not Tested	0.0018
		Max $K_{p/m}$ (cm/s)	2.39E-02	1.67E-02	1.68E-02	Not Tested	1.51E-03
	5°	Max Q_{Mean} (m^3/min)	0.0286	0.0214	0.0106	Not Tested	0.0003
		Max $K_{p/m}$ (cm/s)	2.38E-02	1.78E-02	8.82E-03	Not Tested	2.25E-04

It is thus reasonable that as the incline is increased, more water flows further laterally downslope before exiting the pavement at its base, regardless of material selection. This suggest the existence of two components of unsaturated flow within PICP namely; a vertical (FV_{Vert}) and lateral (FV_{Lat}) component, with a resultant component (FV_{Res}) directly downward in the direction of gravity (Figure 9). These components represent the velocity of unsaturated flow in various directions within the pavement. When the incline is small (near horizontal) the data shows that FV_{Lat} is extremely small too and that FV_{Vert} is dominant. When incline is increased, FV_{Lat} becomes larger while FV_{Vert} becomes smaller. Therefore, a critical angle must exist where, if it is further increased, dominance shifts from the FV_{Vert} component to the FV_{Lat} component. Data obtained from the Full-scale Model shows that this angle exists somewhere between 2.5° and 5° or greater, as the sharpest increases in the discharges, regardless of material selection, were measured from points Q_2 to Q_4 and especially in runoff (Q_5) between these angles.

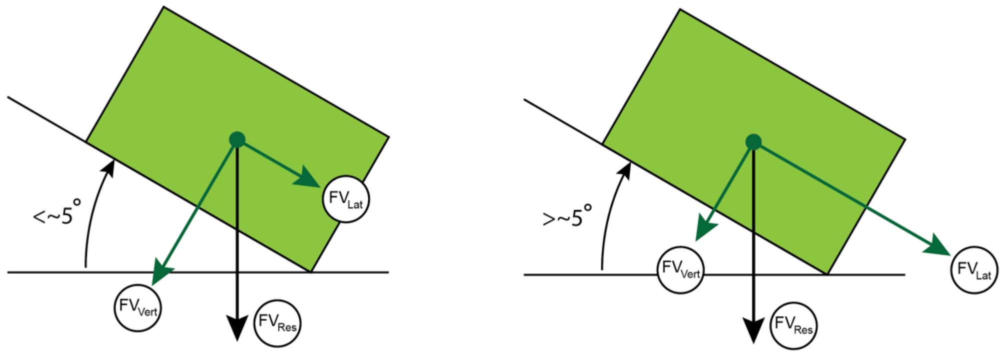

Figure 9. Schematic diagram of the observed flow velocity components in PICP at different inclines.

A possible reason for this behaviour may be the occurrence of capillary barred perching between the SC and the remainder of the layer works at low inclines (Dippenaar and van Rooy, 2019), as the SC generally has a higher density and thus lower permeability than the lower layers of the pavement. In addition, the interface between the SC and lower layers may also simulate the bottom of a horizontal fracture, where lateral flow presents a longer pathways and higher energy requirements (Jones et al., 2018). Water then builds up on the interface, before moving laterally, until enough is present to overcome the adhesion and suction pressures to form a breach allowing downward migration. When incline is increased, the boundary between the SC and the rest of the layer works is no longer horizontal. This results in the migration of water along the boundary by percolation, to areas of the SC with a lower saturation through cohesion and gravity, rather than water crossing the boundary which requires more energy (Dippenaar and van Rooy, 2019).

A clear example of this behaviour is shown in Figure 10 describing a test conducted on the Full-scale Model with a Citylock® and P-Type 3 SC at 0° incline. During this test, the formation of tendrils was noted within the sub-base layers of the model while the layers of the SC were near saturation, demonstrating that flow in the sub-base layers may resemble unsaturated flow between different media resulting in fingering and dispersion plumes as described by Brouwers and Dippenaar (2019). Their formation validated the suspicion that a build up occurs on the boundary between the SC and the lower layers of the pavement until the suction pressures are overcome and a breach is formed. The breach then provides a preferential pathway for further flow to occur by decreasing the invasion pressure at that point giving rise to a stationary and persistent tendril or rivulet.

(a)

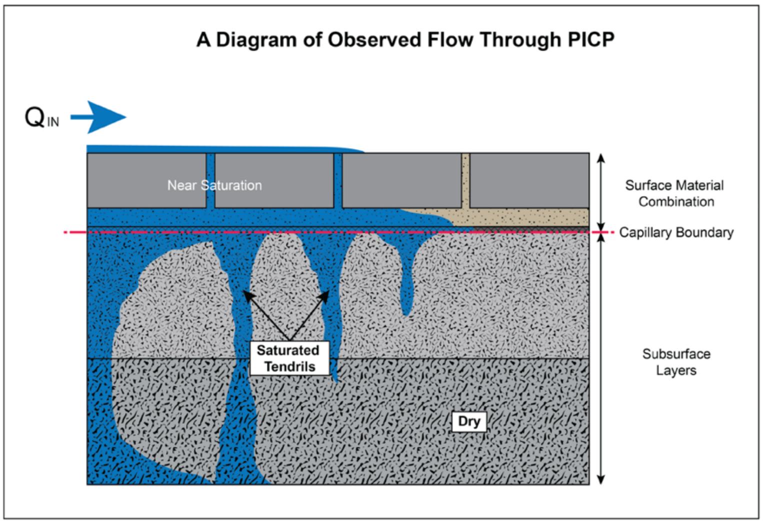

(b)

Figure 10. A (a) tendrils formed in the sub-base layers for Full-scale Model testing of a layer works containing a Citylock® and P-Type 3 sand surface combination at an incline of 2.5° and (b) a schematic representation of the flow mechanisms observed during testing of the Full-scale Model.

5. Conclusions

Apart from the clear evidence that PICP are extremely effective at managing stormwater and water attenuation schemes, it was seen that there are several other benefits to their use in urban developments as well. These benefits include their ability to accommodate large amounts of flow which may occur over a long period of time or instantaneously, that they can retard the flow of water within their layer works and that a large amount of attenuation can be achieved by a very small area of pavement. The benefits associated with PICP are however, subject to some key factors and will only be present if proper design and construction procedures are followed.

5.1. Key Findings

- The permeability of PICP will primarily depend on the material properties of their layer works and only partially on their respective thicknesses.
- The permeability of PICP will be determined by that of the lowest permeability layer.
- An increase in incline affects the permeability of PICP. A steeper incline will induce more interflow, resulting in a decrease in permeability while a lower incline will induce percolation.
- A typical Type-A PICP will have a maximum mean infiltration rate of 0.0407 m^3/min or 3.39E-02 cm/s, if it is not limited by a low permeability subgrade, which is subject to decrease to around 0.0286 m^3/min or 2.38E-02 cm/s when it is constructed on an incline or slope of 5° or 7.8%;
- There exists an angle above 5° where lateral flow will dominate and PICP will no longer have satisfactory performance.
- The orientation of the joints between the bricks in the surface layer does not affect the permeability or performance of PICP.

5.2. Limitations and Assumptions

Every effort was made to complete this study in a representative and accurate manner but the time and budget constraints of the project necessitated the use of certain assumptions. Firstly, it was assumed that all Waterwise® and Citylock® brick units were identical to the other units of their product range in every way. Secondly it was assumed that the ambient atmospheric conditions at the time of each test, such as temperature, humidity, atmospheric pressure etc., had no effect on the outcome of the test. Thirdly, it was assumed that the chosen layer works of the Full-scale Model and the variations thereof, were accurate representations of actual PICP constructed in industry. Lastly, it was assumed that the deck had negligible effect on the hydraulic properties of the model.

In addition, there were some limitations to the Full-scale Model. The first was that the model did not investigate the phenomenon of clogging and its effect on the performance of PICP. Clogging is an intensely complex process and falls beyond the reach of this study's scope as well as its budget and time constraints. It would be better understood through a study dedicated to it alone. The second limitation was that the Full-scale Model only investigated the hydraulic properties of PICP subjected to sheet flow. A system that could wet the pavement within the ITA in a way that simulated rainfall would have been invaluable to this study but unfortunately also fell outside of the time constraints.

5.3. Way Forward

In the context of the global initiative for urban developments to be more environmentally friendly and particularly in terms of water conservation in South Africa, PICP are extremely effective, efficient and there is vast potential for their application and future development. While this study only provides data for these pavements in a selection of conditions, it will certainly assist industry and design professionals. With more studies such as this, the hope is that enough information will be available for the creation of an internationally accepted set of standards and for PICP design and construction.

6. Acknowledgements and Declarations

Acknowledgement is expressed to the South African Water Research Commission (www.wrc.org.za) for funding of project K5/2826 on *Vadose Zone Hydrology: Complexity and Anthropogenic Influences*, as well as to Bosun Concrete Products (Pty) Ltd for the construction, supply and maintenance of the Infiltration Table Apparatus and experimental materials.

Numerous people contributed to discussions about typical pavement designs and testing parameters. Too many to mention, they helped define the test parameters to mimic actual design criteria as closely as possible.

The authors declare no conflicts of interest.

7. References

Addis, B. (2001), Chapter 1, Cementius Material. In: Addis, B. and Owens, G. Fulton's concrete technology 8th Ed. Cement and concrete institute, Midrand.

Addis, B. (2001), Chapter 7, Strength of hardened concrete. In: Addis, B. and Owens, G. Fulton's concrete technology 8th Ed. Cement and concrete institute, Midrand.

Addis, B. (2001), Chapter 11, Concrete Mix Design. In: Addis, B. and Owens, G. Fulton's concrete technology 8th Ed. Cement and concrete institute, Midrand.

Alexander, M. (2001), Chapter 8, Deformation and volume change of hardened concrete. In: Addis, B. and Owens, G. Fulton's concrete technology 8th Ed. Cement and concrete institute, Midrand.

ASTM C29 (2009), Standard Test Method for Bulk Density and Voids In Aggregate.

ASTM C1688 (2013), Standard Test Method for Density and Void Content of Freshly Mixed, Pervious Concrete.

ASTM C1701/C1701M-09 (2009), Standard Test Method for Infiltration Rate of In Place 1 Pervious Concrete, ASTM International, West Conshohocken, PA, 2009.

ASTM C1754 (2012), Standard Test Method for Density and Void Content of Hardened, Pervious Concrete.

ASTM C1781 (2013), Standard Test Method for Surface Infiltration Rate of Permeable Unit Pavement Systems.

ASTM D2434 (2006), Standard Test Method for the Permeability of Granular Soils (Constant Head).

ASTM D3385 (2009), Test Method for Infiltration Rate of Soils In Field Using Double-Ring Infiltrometers.

ASTM D5084 (2010), Standard Test Methods for Measurement of Hydraulic Conductivity of Saturated Porous Materials Using a Flexible Wall Permeameter.

Ballim, Y. and Basson, J. (2001), Chapter 9 Durability of concrete. In: Addis, B. and Owens, G. Fulton's concrete technology 8th Ed. Cement and concrete institute, Midrand, pp 135 – 161.

Bean, E. Z., Hunt, W. F., & Bidelspach, D. A. (2007). Evaluation of four permeable pavement sites in eastern North Carolina for runoff reduction and water quality impacts. Journal of Irrigation and Drainage Engineering, 133, 583–592.

Bean, E. Z., Hunt, W. F., & Bidelspach, D. A. (2007). Field Survey of Permeable Pavement Surface Infiltration Rates. Journal of Irrigation and Drainage Engineering, 2007 pp. 249-255.

Beeldens, A., and Herrier, G., (2006), Water pervious pavement blocks: The Belgian experience, 8th International Conference on Concrete Block Paving, November 6-8, 2006 San Francisco, California USA.

Bosman, R. (2017), Critical water shortages disaster plan - Public Summary, Safety and Security Department, City of Cape Town, www.capetown.gov.za/thinkwater .

Bosun Brick (Pty) Ltd., (2017-2019), No. 9 Cresset Rd, Choolorkop, Edenvale, 1624.

Boyd, K. (No Date), Crushing Plant Design and Layout Considerations, Material Handling, AMEC Mining & Metals, Vancouver.

Brouwers, L. B. and Dippenaar, M. A., (2019), Partially saturated flow from sand into a discrete smooth open vertical fracture at the soil–rock interface: experimental studies, Bulletin of Engineering Geology and the Environment, Springer-Verlag GmbH Germany.

Cairns, J. C. (2012), A Step-by-step Guide to Perfect Paving, Concrete Manufacturers Association NPC, Isikhova Publishing & Communications, Johannesburg. Available from https://issuu.com/precast/docs/step_by_step

Cairns, J. C. (2009), Chapter 22, Precast Concrete Products. In: In: Addis, B. and Owens, G. Fulton's concrete technology 8th Ed. Cement and concrete institute, Midrand.

Castro, D., Gonzalez-Angullo, N., Rodríguez, J. and Calzada, M., (2007), The influence of paving-block shape on the infiltration capacity of permeable paving. Land Contamination and Reclamation 15 Vol. 3, pp. 335-344.

Concrete. (2011). Encyclopædia Britannica. Encyclopædia Britannica Ultimate Reference Suite. Chicago: Encyclopædia Britannica.

Department for Environment, Food and Rural Affairs (DEFRA), (2011), National Standards for sustainable drainage systems, Designing, constructing, operating and maintaining drainage for surface runoff, DEFRA, Area 2A, Ergon House, London.

Dippenaar, M. A., and van Rooy, L. J., (2019), Vadose Zone Characterisation for Hydrogeological and Geotechnical Applications, IAEG/AEG Annual Meeting Proceedings, San Francisco, California, 2018, Vol. 2.

Domone, P. and Illston, J., (2010), Construction Materials: Their nature and behaviour, 4th Ed., Spon Press, London.

EN 1097-3 (1998), Tests for mechanical and physical properties of aggregates, Determination of loose bulk density and voids.

Fassman, E. A., and Blackbourn, S., (2010), Urban Runoff Mitigation by a Permeable Pavement System over Impermeable Soils, Journal of Hydrologic Engineering, ASCE, 2010, pp. 475-485.

Ferguson, B. K., (2006), Porous pavements: The making of progress in technology and design, 8th International Conference on Concrete Block Paving, November 6-8, 2006 San Francisco, California USA.

Gonzalez de Vallejo, L. I. and Ferrer, M. (2011), Geological Engineering, CRC Press, Netherlands.

Grieve, G. (2001), Chapter 3, Aggregates for concrete. In: Addis, B. and Owens, G. Fulton's concrete technology 8th Ed. Cement and concrete institute, Midrand.

Hu N., Zhang J., Xia S., Han R., Dai Z., She R., and Cui X, (2020), A Field Performance Evaluation of the Periodic Maintenance for Pervious Concrete Pavement, Journal of Cleaner Production, 263.

Jones, B. R., van Rooy, L. J., and Dippenaar M. A., (2018), On the Differing Role of Contact Obstacles on Variably Saturated Flow in Vertical and Horizontal Fractures, IAEG/AEG Annual Meeting Proceedings, San Francisco, California, 2018, Vol. 4.

Kamali, M., Delkash, M., Tajrishy, M., (2017), Evaluation of permeable pavement responses to urban surface runoff, Journal of Environmental Management, 187, pp. 43-53.

Kelly A., Collins, E. I., William F., Hunt, P.E., Jon M., Hathaway, E. I., (2007), Hydrologic and water quality comparison of four types of permeable pavement and standard asphalt in eastern North Carolina, Interlocking Concrete Pavement Institute, 1444 I Street, NW - Suite 700, Washington, DC.

Kumar, K., Kozak, J., Hundal, L., Cox, A., Zhang, H. and Granato, T., (2015), In-situ infiltration performance of different permeable pavements in a employee used parking lot - A four-year study, Journal of Environmental Management, 167, pp. 8-14.

Kuosa, H., Niemelainen, E. and Korkealaakso, J., (2014), Previous pavement testing methods – State-of-the-art and laboratory and field guideline for performance assessment, Research report VTT-R-08225-13, VTT, Finland.

Lane, J. (2001), Chapter 20, Concrete masonry units and paving blocks. In: Addis, B. and Owens, G. Fulton's concrete technology 8th Ed. Cement and concrete institute, Midrand.

Li, H., Kayhanian, M., and Harvey, J. T., (2013), Comparative field permeability measurement of permeable pavements using ASTM C1701 and NCAT permeameter methods. Journal of Environmental Management, 118, 144–152.

Lian, C. and Zhuge, C. (2010), Optimum mix design of enhanced permeable concrete: an experimental investigation, In: Construction and Building Materials, Vol. 24. pp. 2664-2671.

Lucke, T., Boogaard, F. and van de Ven, F., (2014), Evaluation of a new experimental test procedure to more accurately determine the surface infiltration rate of permeable pavement systems, Urban Planning and Transport Research, Vol. 2, No. 1, pp22-35.

Lucke, T., White, R., Nichols, P. and Borgwardt, S., (2015), A Simple Field Test to Evaluate the Maintenance Requirements of Permeable Interlocking Concrete Pavements, Water 2015 – Open Access Journal, Vol. 7, pp. 2542-2554.

Oberholster, B. (2001), Chapter 10, Alkali-silica reaction. In: Addis, B. and Owens, G. Fulton's concrete technology 8th Ed. Cement and concrete institute, Midrand.

Pavey, M. J. (2019), New South Wales Government Gazette, No. 55 of 31, May 2019.

Powers, J. P., (1992), Construction Dewatering: New methods and applications, 2nd Ed., John Wiley and Sons, New York.

Salberg, D. B. (1997), Surface water drainage: revised designs and maintenance standards, IMIESA, The official journal of the Institution of Municipal Engineering of South Africa, Vol. 22, No. 11, pp. 25-30.

SANS 927 (2007), Precast concrete kerbs, edging and channels.

SANS 1058 (2012), Concrete Block Paving, Standard specification for concrete masonry units.

SANS 1200-MJ (1984), Standardised specification for civil engineering construction – Laying of paving.

South African Pavement Engineering Manual, (2013), Chapter 8: Material Sources, South African National Roads Agency.

Stewart, D. A., (1951), The design and placing of high quality concrete, London: Spon.

Technicrete, (2017), Permeable Paving: Aqua Trojan Slab®, Square® and Aqua Zig-zag®, Technicrete House, Cnr. Main Reef Road and Houtkapper Street, Roodepoort, 1725.

Taylor, P. (2001), Chapter 5, Chemical Admixtures. In: Addis, B. and Owens, G. Fulton's concrete technology 8th Ed. Cement and concrete institute, Midrand.

Torncoro (N.D.), Technical Guide 2: The use and design of concrete bricks and brickwork, Lithotone, Durban.

TRH 14, (1985), Guidelines for road construction materials, Committee of State Road Authorities, Pretoria.

TRH 20, (1990), The structural design, construction and maintenance of unpaved roads, Committee of State Road Authorities, Pretoria.

United States Department of Agriculture (USDA), (2012), Chapter 3: Engineering Classification of Earth Materials, Part 631: National Engineering Handbook, Amend. 55, January 2012.

van Vuuren, J. H., (2020), Unsaturated flow through permeable pavements: An experimental study, MSc dissertation in the field of Engineering Geology, Department of Geology, University of Pretoria, Lynnwood Rd, Hatfield, Pretoria, 0002, pp44-48

Weinert, H. H., (1980), The natural road construction materials of Southern Africa, National Institute for Transport and Road Research, Pretoria.

Woods-Ballard, B., Kellagher, R., Martin, P., Jefferies, C., Bray, R., Shaffer, P., (2007), The SuDS manual, CIRIA C698, Construction industry research and information association (CIRIA), Classic House, 174–180 Old Street, London.

Yin, S., Yang, Y., Zhang, T., Guo, G., Yu, F., (2015), Effect of carbonic acid water on the degradation of Portland cement paste: Corrosion process and kinetics, Construction and Building Materials, School of Materials Science and Engineering, South China University of Technology, Guangzhou.

Zhang, J.,Cui, X., Tang, W., Lous, J., (2017), Approximate simulation of storm water runoff over pervious pavement. International Journal of Pavement Engineering. 18(3):247-259.